Electronic Supplementary Material (ESI) for Materials Chemistry Frontiers.

Supporting Information

Synthesis of $CoSnS_2$ hollow nanocubes with NIR-enhanced chemodynamic therapy and glutathione depletion for synergistic cancer therapy

Xuerui Zhu[a,b], Zhaoyou Chu[b], Benjin Chen[b], Qianqian Jin[a], Xuke Ma[a], Juan Yang[b], Yongxin Jiang[b], Wanni Wang[b,],Zhengbao Zha[a,]*, Haisheng Qian[b,c,]**

[a] *School of Food and Biological Engineering, Hefei University of Technology, Hefei 230009, P. R. China.*

[b] *School of Biomedical Engineering, Research and Engineering Center of Biomedical Materials, School of Basic Medical Sciences Anhui Medical University, Hefei 230032, P. R. China.*

[c] *Anhui Provincial Institute of Translational Medicine, Anhui Medical University, Hefei, Anhui 230032, P. R. China*

Experimental Section

1. Photothermal Effect of CSS.

2.0 mL aqueous solutions of CSS NPs with different concentrations were exposed upon an 808 nm laser (2.0 W cm^{-2}) for 10 min. Then, CSS NPs (125 μg mL^{-1}) aqueous solutions was exposed to different power of 808 nm laser. The photothermal stability of CSS NPs was further evaluated by repeating the laser on/off cycles for five times. The temperature change of CSS NPs solution was recorded at 10 s intervals by an IR thermal camera (Testo 865).

2. Animal model.

Tumor models were established by injecting 4T1 cells subcutaneously into the back of female BALB/c mice (4 and 5 weeks of age). The CSS was injected when the tumor volume reached 50 ~ 100 mm^3. Animal experiments were approved by the ethics committee of Anhui Medical University (approval number: LLSC20210077). All animal-related experimental protocols were performed in accordance with the guidelines of the Association for Laboratory Animal Science and the Center for Laboratory Animal Science of Anhui Medical University.

3. Characterization.

The surface morphologies, phase, fluorescence, optical properties, X-ray diffraction (XRD) and X-ray photoelectron spectra (XPS) of these products were investigated carefully according to our previous protocol or instruments. Photothermal performance, ROS, Hydroxyl radical (·OH) and singlet oxygen ($^1O_2$) detection were studied via our previously reported protocol. All animal experimental protocols were investigated carefully according to our previous protocol or instruments.

Supporting Figures

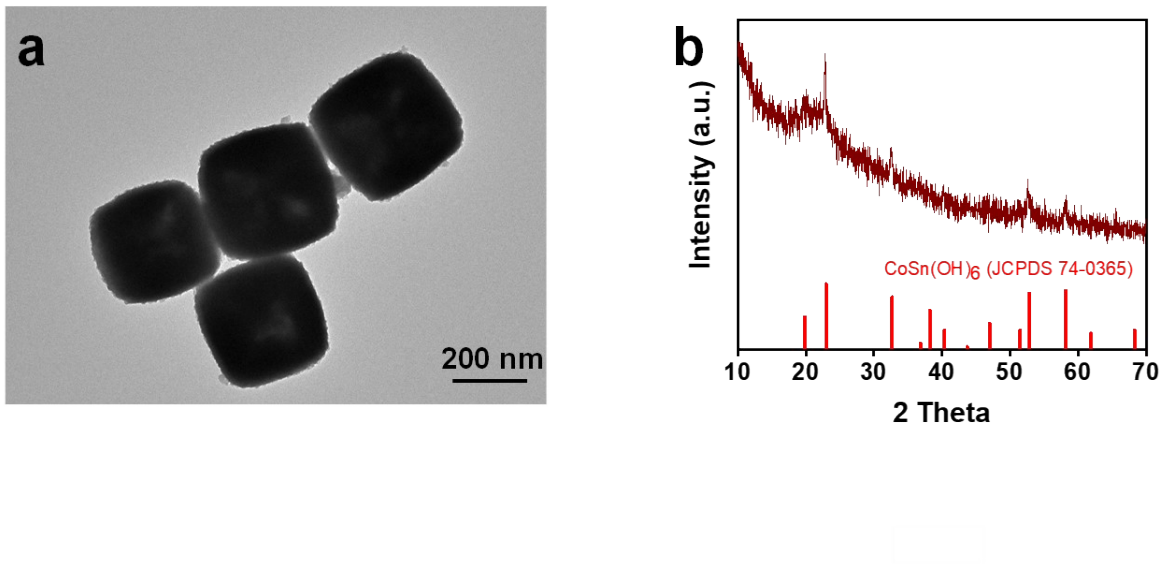

Fig. S1 (a) TEM images of $CoSn(OH)_6$ hollow nanocubes and (b) XRD patterns of as-obtained $CoSn(OH)_6$.

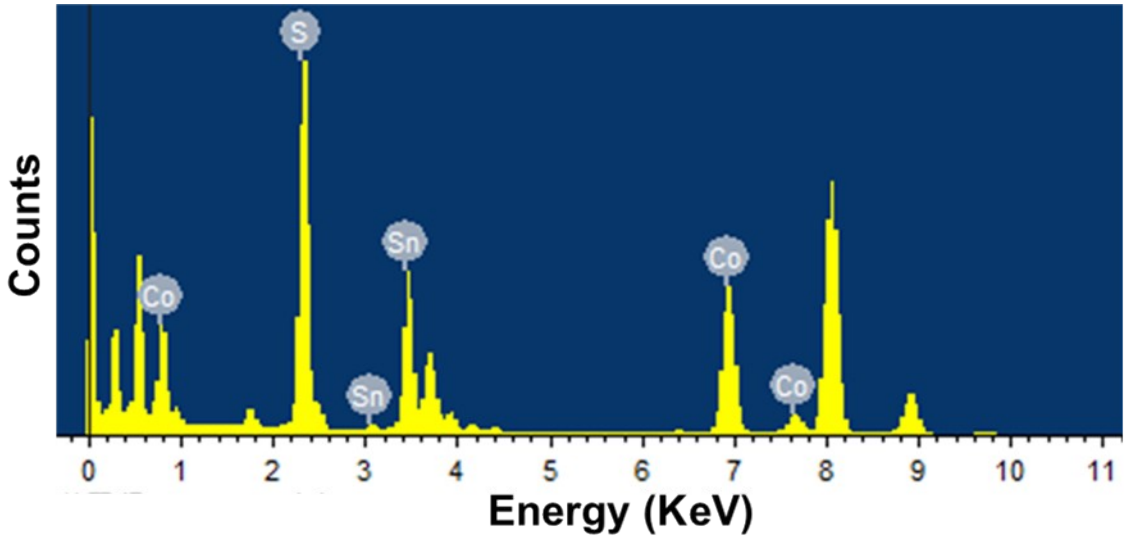

Fig. S2 Energy dispersive X-ray spectra of the as-prepared CSS hollow nanocubes.

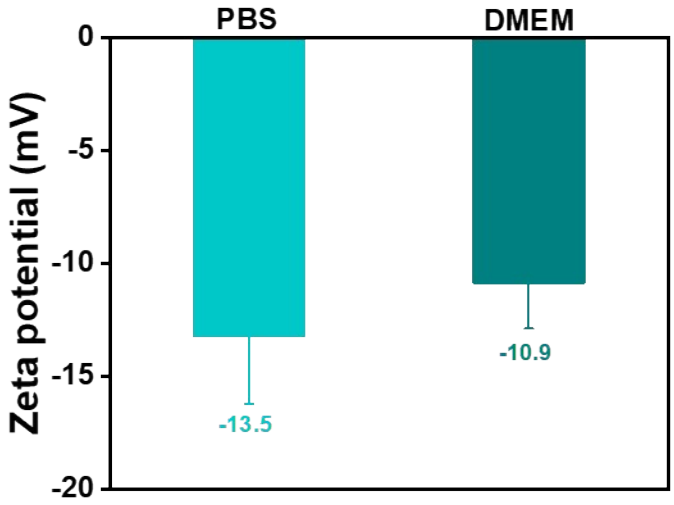

Fig. S3 Zeta potential analyses of CSS dispersed in PBS and DMEM.

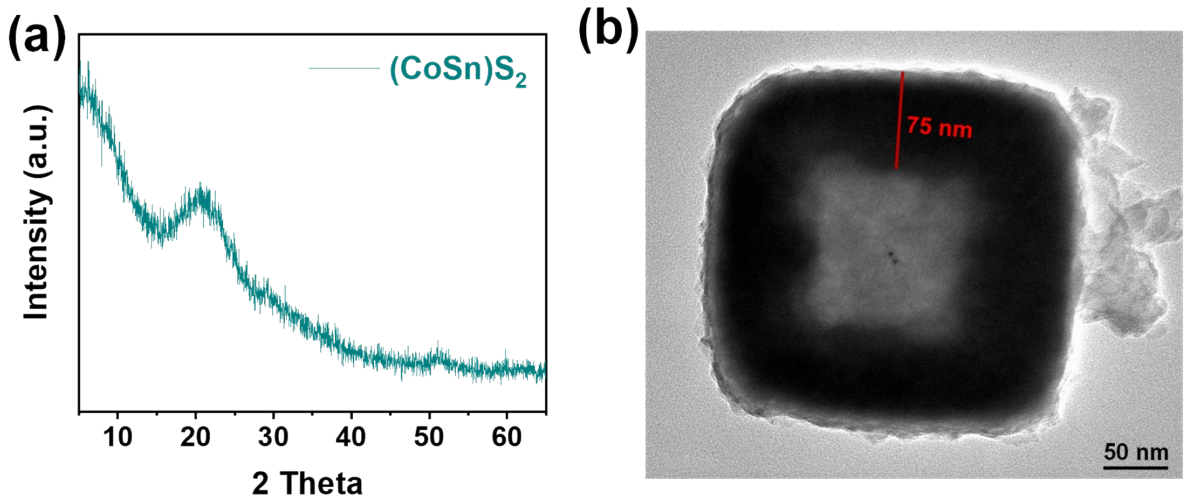

Fig. S4 (a) XRD patterns of as-obtained $(CoSn)S_2$ and (b) TEM images for the single $(CoSn)S_2$ NPs.

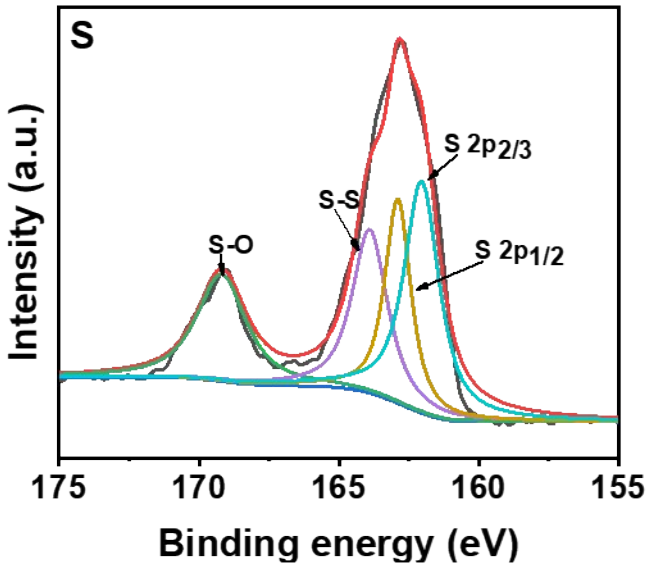

Fig. S5 S XPS spectra of as-obtained CSS.

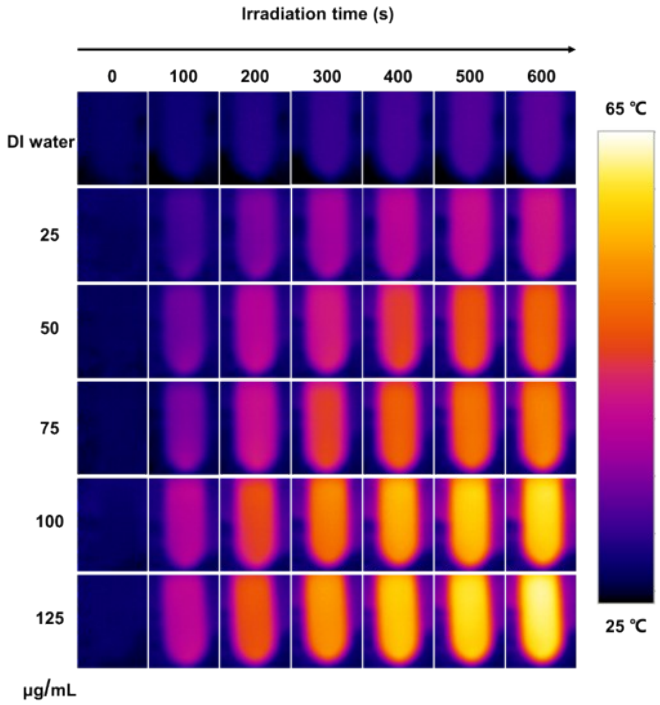

Fig. S6 Thermal images of CSS solutions at various concentrations upon 808 nm laser irradiation (2 W cm^{-2}).

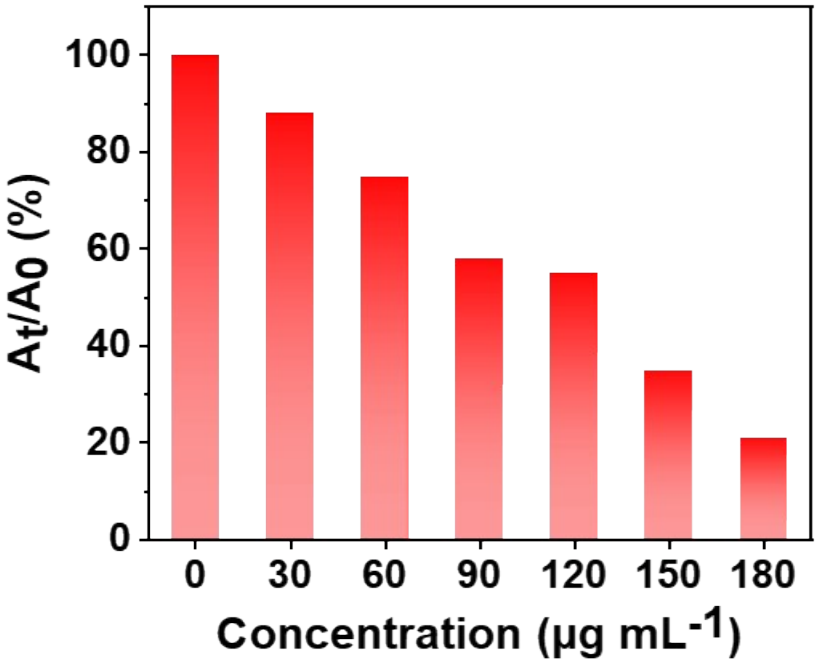

Fig. S7 GSH depletion by CSS at different concentrations characterized by the absorbance of 5,5'-dithiobis-(2-nitrobenzoic acid) (DTNB).

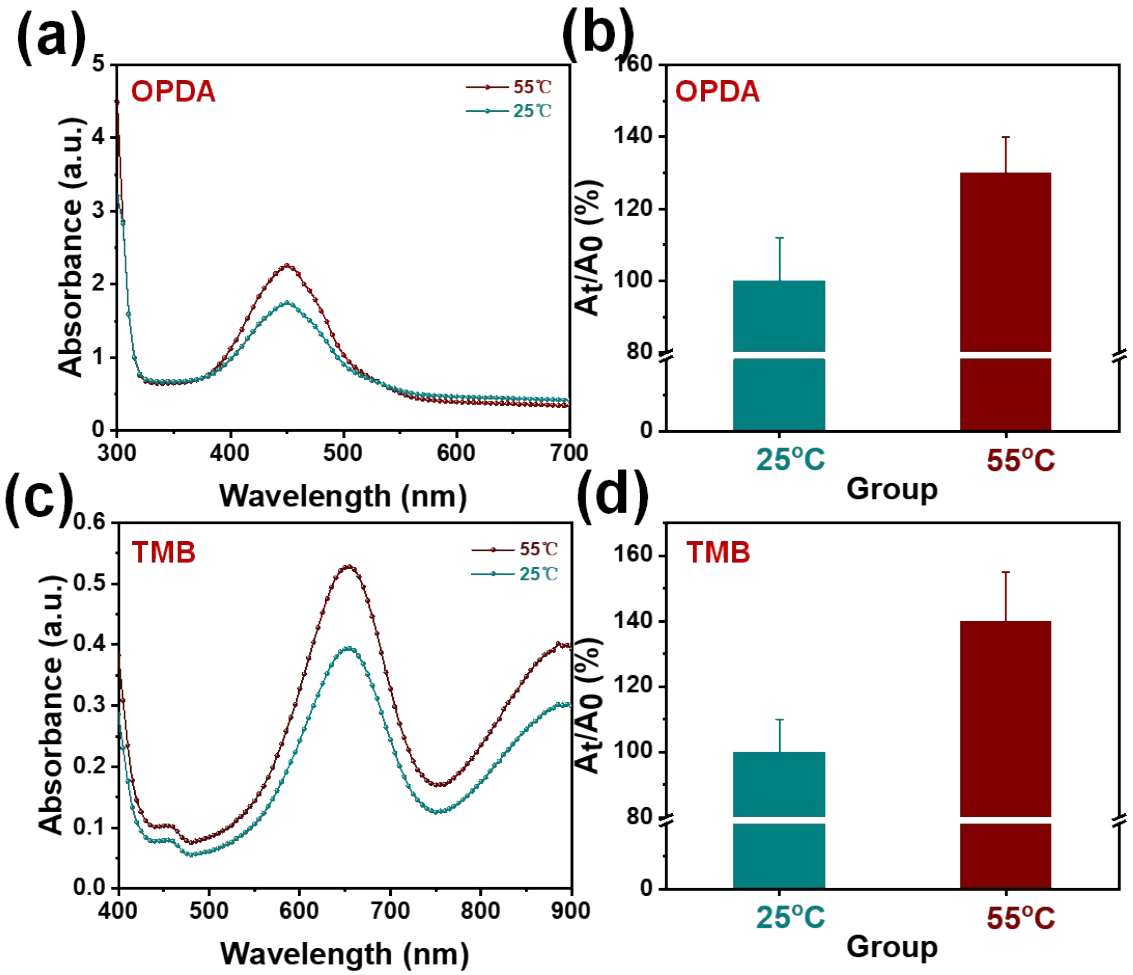

Fig. S8 Fenton catalytic effect of CSSs at different temperature (25°C/55°C) via OPDA and TMB probes.

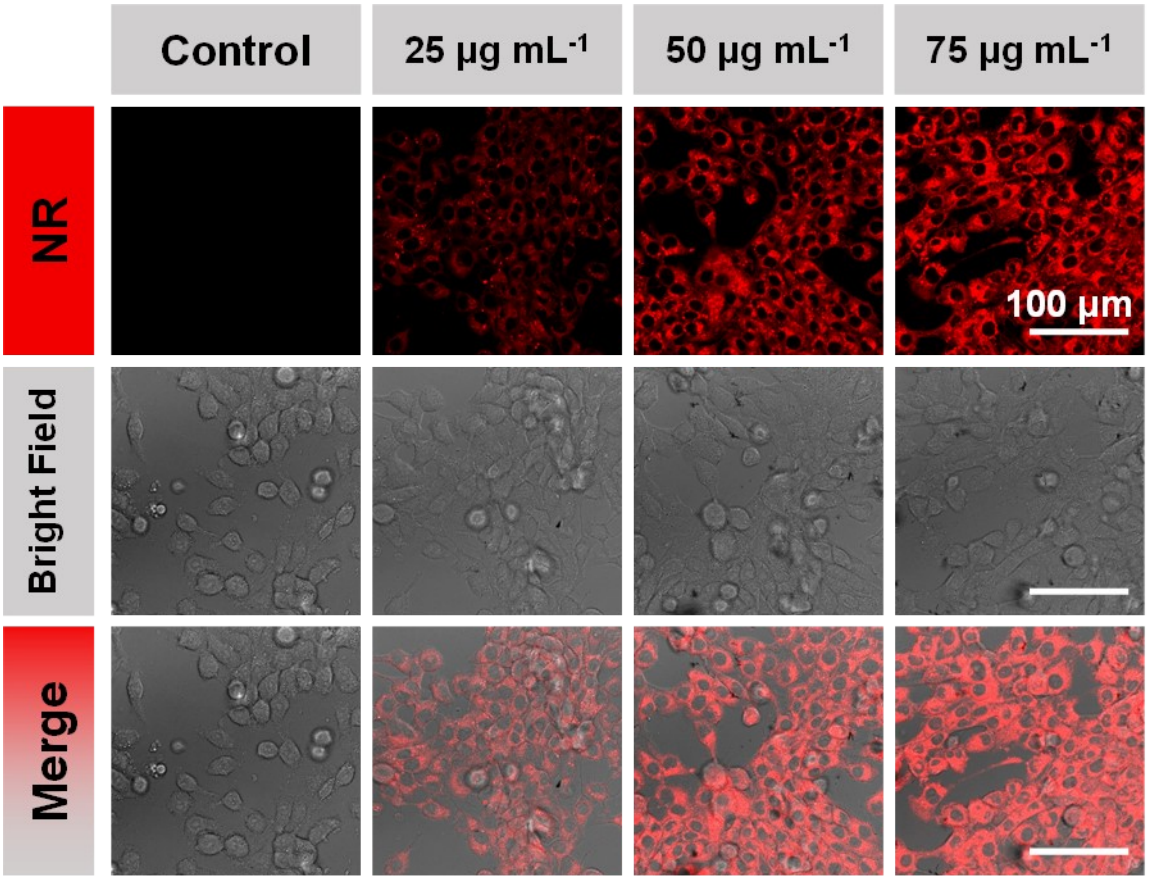

Fig. S9 CLSM images of 4T1 cells after 4 h incubation with CSS at different concentration (0, 25, 50, 75 μg mL^{-1}).

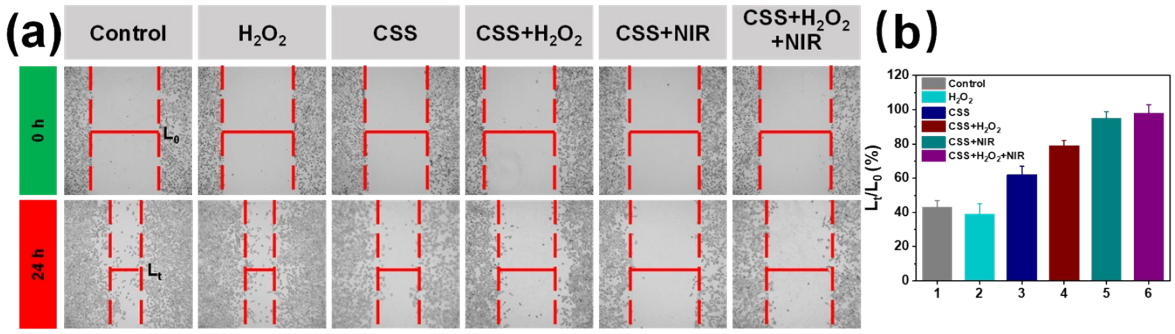

Fig. S10 Results of different experimental groups of the scratching experiment and statistical histogram.

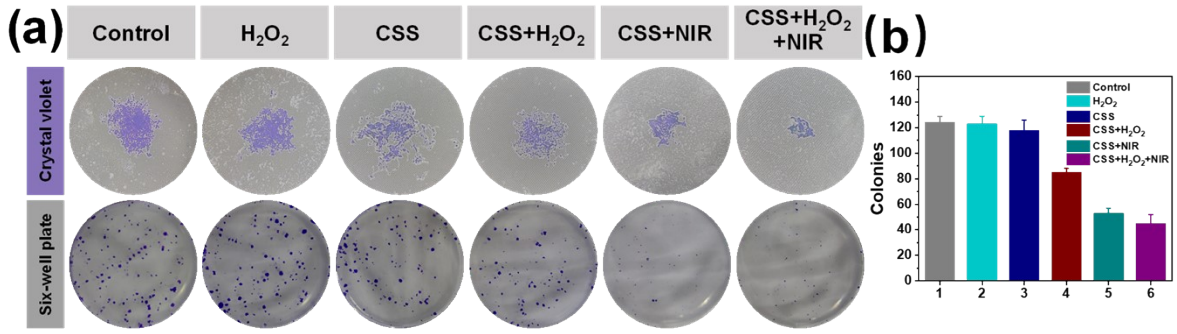

Fig. S11 Results of different experimental groups of plate cell clone formation experiments and statistical histograms.

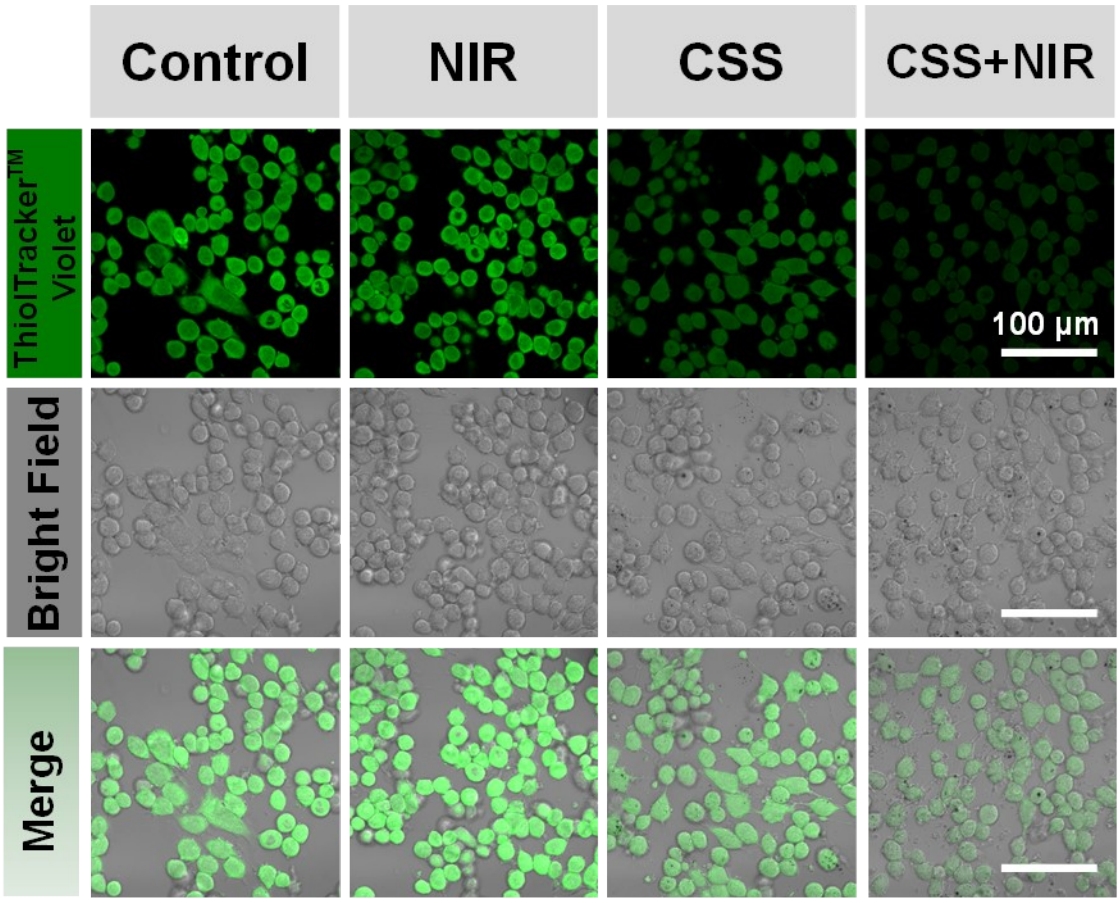

Fig. S12 CLSM images of 4T1 cells for GSH analysis stained by Thiol-Tracker™ Violet after ncubation with different groups.

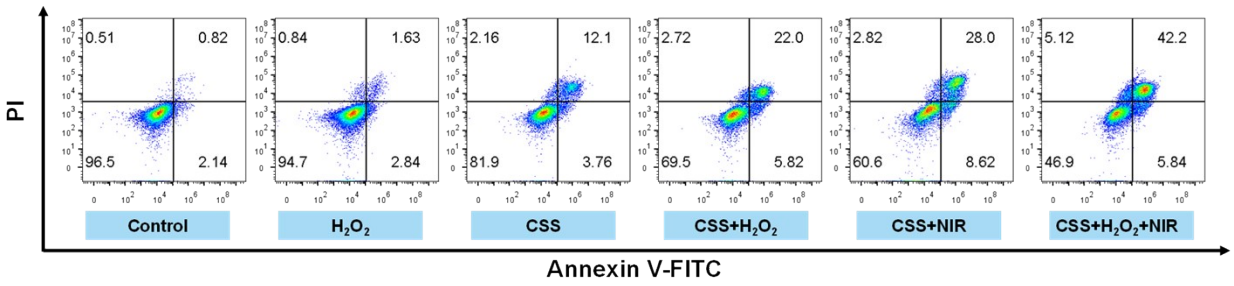

Fig. S13 Flow cytometric analysis of 4T1 cells apoptosis induced by different treatments with Annexin V-FITC/PI staining.

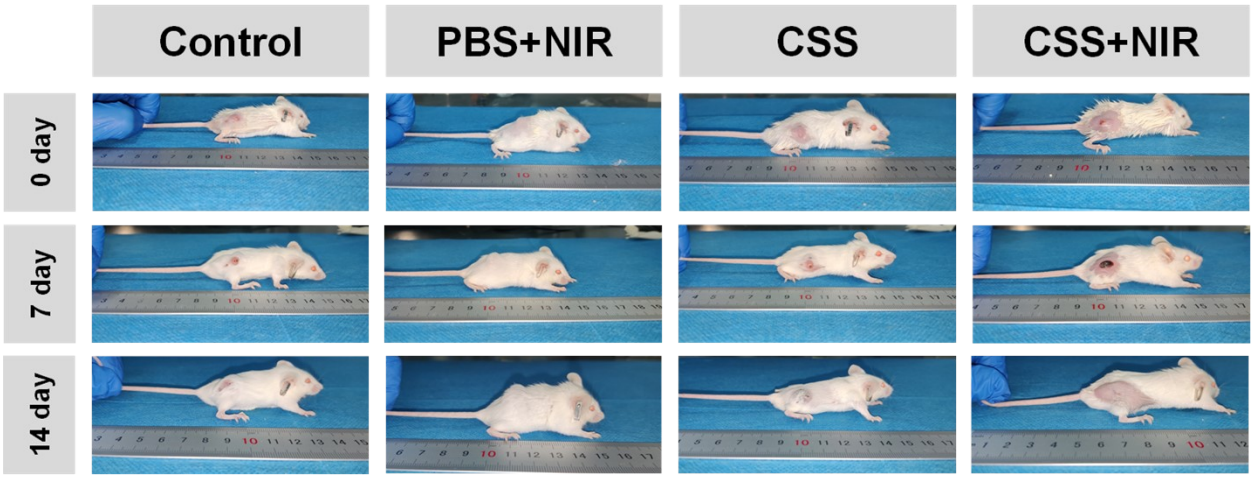

Fig. S14 Representative mice from different treatment groups.

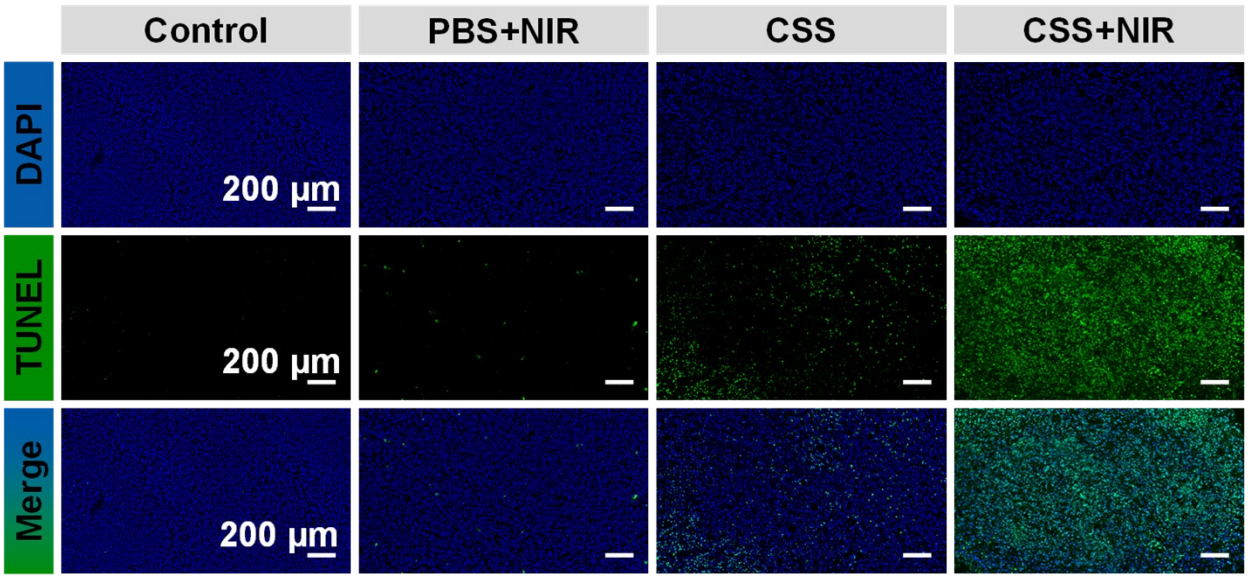

Fig. S15 TUNEL staining images of excised tumors of different treatments group on the 14th day.

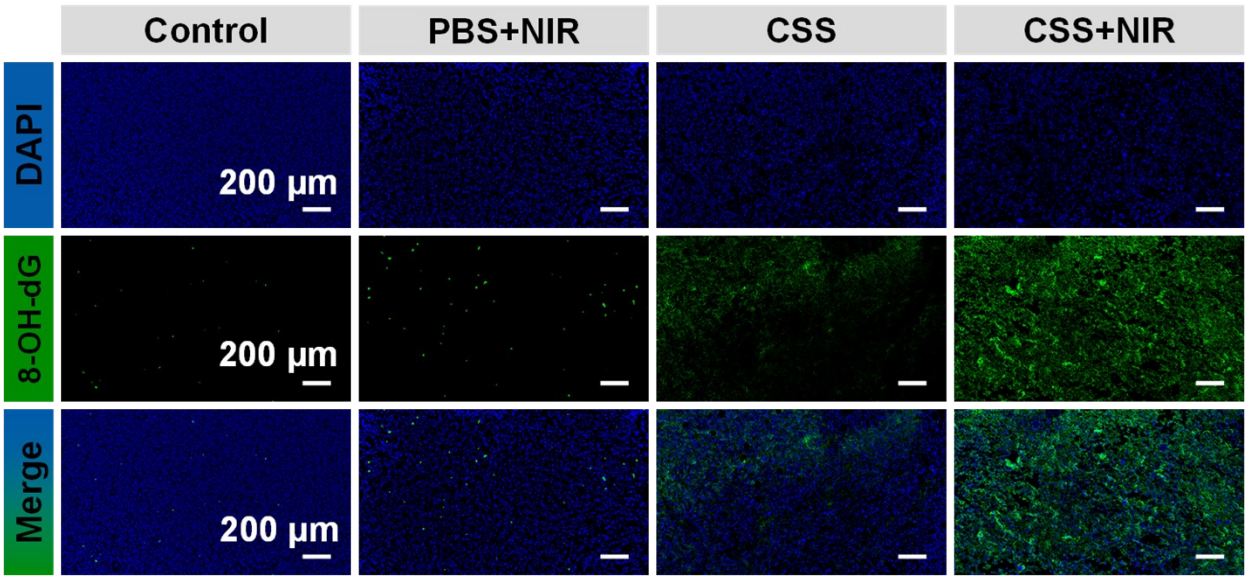

Fig. S16 8-OH-dG staining images of excised tumors of different treatments group on the 14th day.

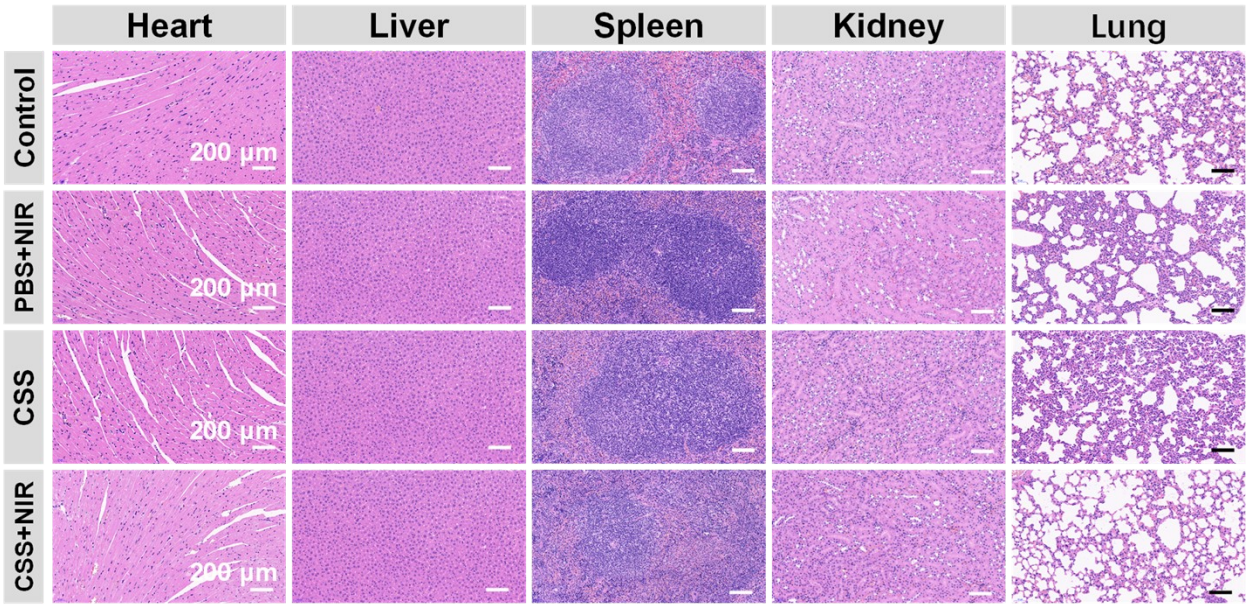

Fig. S17 Hematoxylin and eosin (H&E) stained images of major organs (heart, liver, spleen, kidney, and lung) of mice post-injection of CSS nanoparticles.

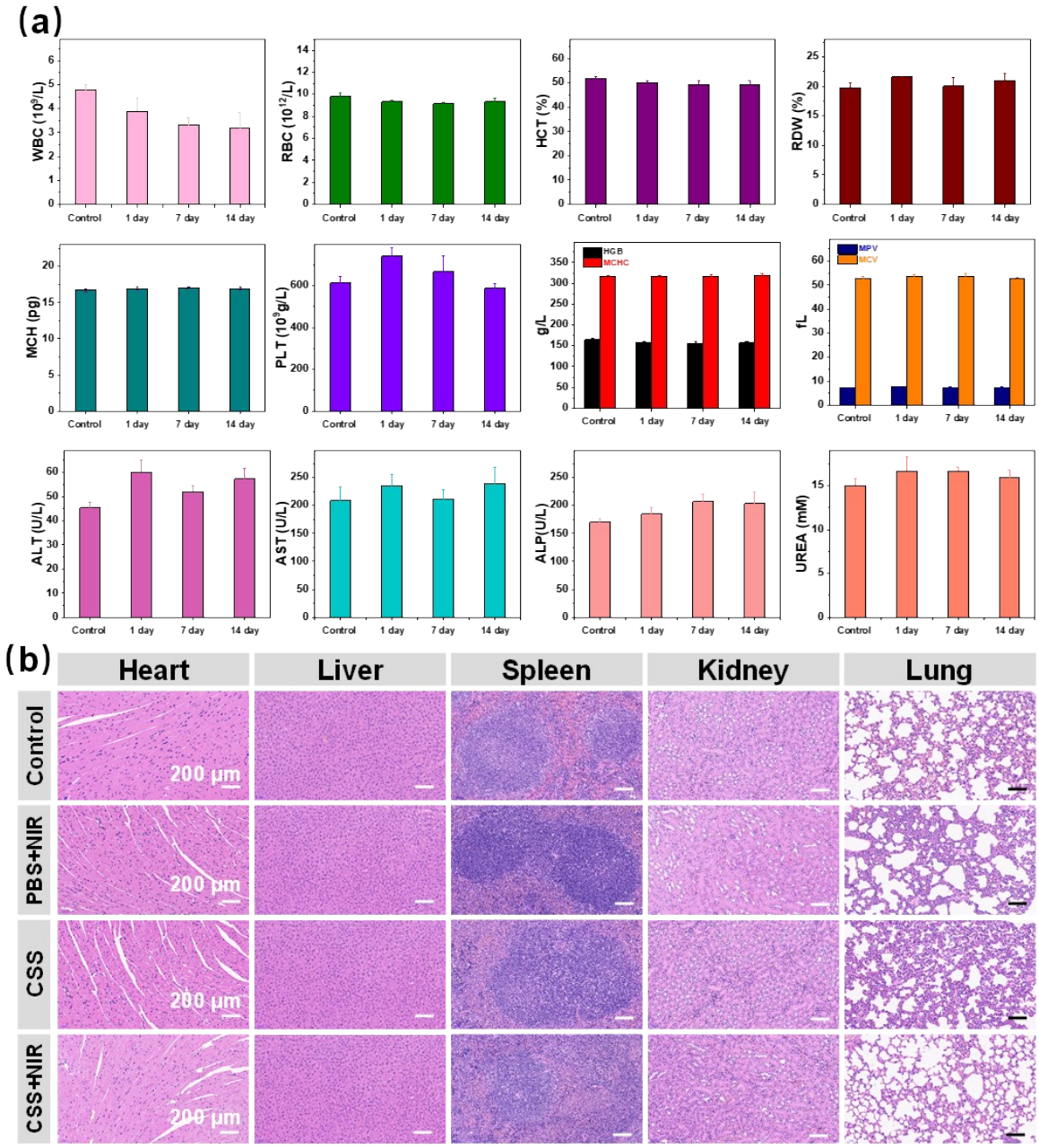

Fig. S18 *In vivo* toxicology assays of the CSS. (a) blood panel analysis and blood biochemistry test of healthy mice after intravenous injection of CSS NPs (10 mg kg^{-1}) at different days. (b) H&E staining images of major organs (heart, liver, spleen, kidney, lung) of the mice after injection of CSS at different time.

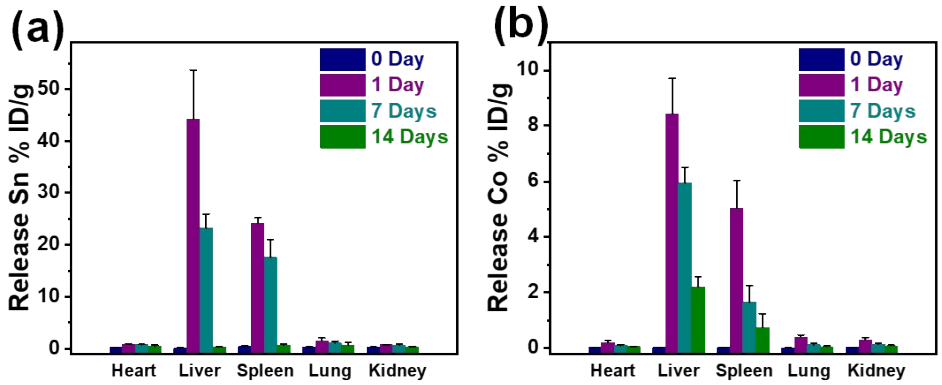

Fig.S19 Ion distribution in the main organs (heart, liver, spleen, lung and kidney) on 0, 1, 7 and 14 days (a) *In vivo* distribution of tin ions (b) *In vivo* distribution of cobalt ions.

Table S1 Element scale in CSS by energy dispersive X-ray spectra.

Element	Weight %	Atomic %
S K	30.24	54.55
Co K	23.20	22.77
Sn K	46.56	22.69
Total	100.00	100.00